

RUB-TPII-56/93  
December, 1993

# Electromagnetic nucleon properties and quark sea polarization in the Nambu-Jona-Lasinio model

A.Z. GÓRSKI<sup>1,2</sup>, CHR.V. CHRISTOV<sup>1</sup>, K. GOEKE<sup>1</sup>

<sup>1</sup> Institute für Theoretische Physik II, Ruhr-Universität Bochum, D-44780 Bochum, Germany

<sup>2</sup> Institute of Nuclear Physics, Radzikowskiego 152, 31-342 Cracow, Poland

## ABSTRACT

In this paper we present the derivation as well as the numerical results for all electromagnetic form factors of the nucleon within the semibosonized Nambu–Jona-Lasinio (chiral quark soliton) model. Other observables, namely the nucleon mean squared radii, the magnetic moments and the nucleon– $\Delta$  splitting are also computed. The calculation has been done taking into account the quark sea polarization effects. The final results, including rotational  $1/N_c$  corrections, are compared with the existent experimental data and they are found to be in a good agreement for the constituent quark mass of 400–420 MeV.

## 1. Introduction

In the last years the most challenging problem in elementary particle physics seems to be solution of QCD in the low energy region. The main difficulties are due to the non-perturbative effects caused by growing effective coupling constant of the fundamental theory in the low energy limit. This prevents one from using the well-known main tool of theoretical physics — the perturbation theory. Because of this, the most intriguing features of QCD — confinement and chiral symmetry breaking — still remain conceptual and practical problems.

The above mentioned obstacles have initiated an increasing interest among the physicists in non-perturbative methods and effective low-energy models of hadrons. The effective models are expected to mimic the behaviour of QCD at energies below  $\sim 1\text{ GeV}$  (confinement and/or chiral symmetry breaking) and to reproduce experimental data in this region. In principle, those models could be related to QCD by integrating out gluonic fields and reparameterizing fermionic degrees of freedom (the bosonization procedure). In effect, the physically observed particles should appear as fundamental fields of the model.

One of the first models of this type that has become very popular was the Skyrme model [1]. It is an example of a fully bosonized effective model. During many years of intensive investigations the Skyrme model has proven to be theoretically quite interesting, though comparison with experiment has not always been good.

The simplest purely fermionic Lorentz invariant model with spontaneous chiral symmetry breaking is the Nambu–Jona-Lasinio (NJL) model [2] that has followed the example of the BCS model of superconductivity. It contains chirally invariant local four-fermion interaction terms and it is non-renormalizable in 4-dimensional space-time. The NJL Lagrangian in its simplest  $SU(2)$  form has the following structure:

$$\mathcal{L}_{NJL} = \bar{q} (i\partial - m_0) q + \frac{1}{2} G [ (\bar{q}q)^2 + (\bar{q}i\vec{\tau}\gamma_5 q)^2 ] , \quad (1)$$

where  $G$  is the coupling constant,  $m_0$  is the current quark mass and  $\vec{\tau}$  are the Pauli matrices in the isospin space. Usually *up* and *down* quarks are assumed as degenerated in mass.

The NJL model is generally solved after applying the well known bosonization procedure following Eguchi [3] to arrive at the model expressed in terms of physically observed particles' fields  $\sigma(\vec{x}), \vec{\pi}(\vec{x})$ :

$$\mathcal{L}'_{NJL} = \bar{q} [ i\gamma^\mu \partial_\mu - g(\sigma + i\vec{\pi}\vec{\tau}\gamma_5) ] q - \frac{1}{2} \mu^2 (\sigma^2 + \vec{\pi}^2) + (m_0 \mu^2/g) \sigma . \quad (2)$$

The new coupling constant  $\mu^2$  is related to the initial  $G$  by:  $G = g^2/\mu^2$ . Here,  $g$  is the physical pion–quark coupling constant implying that  $\vec{\pi}$  are the physical pion fields. The meson fields are constrained to the chiral circle to reproduce the pion decay constant:

$$\sigma^2(\vec{x}) + \vec{\pi}^2(\vec{x}) = f_\pi^2 , \quad (3)$$

where  $f_\pi = 93\text{ MeV}$  is the pion decay constant.

In fact, an equivalent effective chiral quark meson theory [4,5] can be derived from the instanton model of the QCD vacuum.

In the chiral quark soliton model [5-7] based on the lagrangean (2) (frequently reffered simply as NJL model) the baryons appear as a bound state of  $N_c$  valence quarks coupled to the polarized Dirac sea ( $\bar{q}q$ ). Operationally the baryon sector of the model is solved in two steps. In the first step, motivated by the large  $N_c$  limit, a static localized solution (soliton) is found. It is done by solving the equations of motion in an iterative selfconsistent procedure assuming that the  $\sigma$  and  $\vec{\pi}$  fields have hedgehog structure. However, this hedgehog soliton does not preserve the spin and isospin. In order to describe the nucleon properties one needs nucleon states with the proper spin and isospin numbers. To this end the classical solution is semiclassically quantized making use of the rotational zero modes. In fact, such a cranking procedure was elaborated in [5]. Recently, within this scheme including Dirac sea polarization effects quite successful calculations for the nucleon moment of inertia [13], magnetic moments [14] and nucleon electric form factors [15] have been reported.

There are several reasons that the model described by (5) is considered as one of the most promising effective theories describing low energy QCD phenomena. First, the model is the simplest quark model which provides mechanism for spontaneous breaking of the chiral symmetry — the very basic feature of QCD. The mesons appear as excited states of quark-antiquark pairs. The philosophy behind this approach is based on the hypothesis that the chiral symmetry breaking and confinement are relatively independent mechanisms and they can be investigated separately [5].

Second, the self-consistent solitonic solution (*hedgehog*) has been found to exist in the large  $N_c$  limit of the model within the physically acceptable range of parameters [7]. The chiral soliton provides a good description of the nucleon and gives us possibility to take into account vacuum polarization effects from the Dirac quark sea. Calculations done in the semiclassical quantization procedure yield quite reasonable results for the vacuum and nucleon sectors [8-10]. In particular, quantities like the nucleon radii,  $\Sigma$ -terms, axial vector coupling constant,  $\Delta$ -nucleon splitting, splittings within the octet and decuplet are well reproduced.

Third, there are various hints that the NJL-type Lagrangian can be obtained [4,5,11,12] as a long wavelength limit of QCD. It should be stressed that the large  $N_c$  limit plays a prominent role in those considerations.

The aim of this paper is to compute the electromagnetic nucleon form factors within the  $SU(2)$  chiral quark soliton model based on the semibosonized NJL-type lagrangean with the vacuum polarization effects taken into account. The calculations will include the rotational  $1/N_c$  corrections, which really have been shown to be important for the isovector magnetic moment. Calculations of this sort give us possibility to calculate all electromagnetic properties of nucleons, as well as such quantities like the electric mean squared radii, the magnetic moments, the nucleon– $\Delta$  energy splitting, and the electric and magnetic charge distributions.

The paper is organized as follows: we begin in Sec. 2 with formulation of the regularized model, introduction of the rotational zero modes and we derive expression for the electromagnetic current treating the angular velocity as a perturbation. In Section 3 we derive the analytical expressions for the form factors including terms up to the linear order in angular velocity. Section 4 is devoted to presentation of numerical results. Summary and discussion is given in the last section.

## 2. The regularized action and current

In Minkowski space the generating functional of the model written in terms of the quark and meson fields,  $\sigma(\vec{x}), \vec{\pi}(\vec{x})$  has the form:

$$Z'_{NJL} = \int \mathcal{D}\bar{q}\mathcal{D}q\mathcal{D}\sigma\mathcal{D}\vec{\pi} \exp \left[ i \int d^4x \mathcal{L}'_{NJL}(x) \right], \quad (4)$$

The sources are not explicitly included.

Since the NJL model is a non-renormalizable theory, a regularization scheme of an appropriate cut-off  $\Lambda$  is needed to make the theory finite. To this end we will work in Euclidean space-time (the conventions used are given in the Appendix).

After Wick rotation (transformation to the Euclidean space-time) integrating out the quarks in (4) one gets the effective action split in fermionic and mesonic parts:

$$S_{eff} = S_{eff}^F + S_{eff}^M + S_{eff}^{br}, \quad (5)$$

The fermionic part of the action includes the quark loop contribution in the presence of the external meson fields  $(\sigma, \vec{\pi})$ :

$$S_{eff}^F = -\text{Sp} \ln(\not{D}_E). \quad (6)$$

The Dirac operator  $\not{D}_E$  (in Euclidean space-time) has the form:

$$\not{D}_E = \gamma_4 [\partial_4 - h(U)]. \quad (7)$$

with the one particle Hamiltonian operator  $h_E$  defined as

$$h_E(U) \equiv i [-i \gamma_4 \gamma_k \partial_k + \gamma_4 M U]. \quad (8)$$

The constituent quark mass  $M = g f_\pi$  and

$$U = \frac{1}{f_\pi} (\sigma + i \gamma_5 \vec{\tau} \vec{\pi}) \quad (9)$$

represents the mesonic fields. It can be checked by inspection that the Hamiltonian is Hermitian:  $(h_E)^\dagger = h_E$ .

The mesonic part

$$S_{eff}^M = \frac{\mu^2}{2} \int d^4 x_E (\sigma^2 + \vec{\pi}^2), \quad (10a)$$

and

$$S_{eff}^{br} = -\frac{m_o \mu^2}{g} \int d^4 x_E \sigma, \quad (10b)$$

includes an explicit symmetry breaking term (10b).

In order to compute the electromagnetic current matrix elements we include the electromagnetic coupling in a minimal way and we take into account the rotational zero modes.

We start with the Dirac operator  $\not{D}_E$  with electromagnetic potential  $A_\mu$ :

$$\not{D}_E = \gamma_4 \left[ \partial_4 - h(U) - i A_4 \hat{Q} + i \gamma_4 \gamma_k A_k \hat{Q} \right], \quad (11)$$

The quark charge matrix  $\hat{Q} \equiv \frac{1}{6} \hat{1} + \frac{1}{2} \tau^3$ .

In the next step, we introduce the rotating soliton:

$$\tilde{U}(\vec{x}, x_4) \equiv R(x_4) \bar{U}(\vec{x}) R^\dagger(x_4), \quad R \in SU_2, \quad R^\dagger R = \hat{1}. \quad (12)$$

where the meson field  $\bar{U}(\vec{x})$  corresponds to the stationary point (minimum) of the effective action (5). In the Euclidean space-time the rotation matrix  $R(x_4)$ , can be represented as:

$$R(x_4) = \exp(-ix_4 \Omega), \quad \Omega \equiv \frac{1}{2} \tau^A \Omega^A \quad \text{and} \quad \Omega_E = -i R^\dagger \dot{R}, \quad (13)$$

where as usually the summation convention over repeated indices is assumed.

In body-fixed frame the Dirac operator of the rotating soliton  $\tilde{\mathcal{D}}_E(\bar{U})$  can be expressed in the form:

$$\tilde{\mathcal{D}}_E(\bar{U}) = R^\dagger \mathcal{D}_E(\tilde{U}) R , \quad (14)$$

where  $\tilde{\mathcal{D}}_E$  is defined by:

$$\tilde{\mathcal{D}}_E(\bar{U}) = \gamma_4 \left[ \partial_4 - h(\bar{U}) + i\Omega - iA_4 R^\dagger \hat{Q}R + i\gamma_4 \gamma_k A_k R^\dagger \hat{Q}R \right] . \quad (15)$$

The operator  $\Omega$  is Hermitian in both, Euclidean and Minkowski space-time:

$$\Omega_E^\dagger = \Omega_E, \quad \Omega_M^\dagger = \Omega_M . \quad (16)$$

Taking into account (A.1) and (16) we can write down the Hermitian conjugate to (15):

$$\tilde{\mathcal{D}}_E^\dagger(\bar{U}) = \left[ -\partial_4 - h(\bar{U}) - i\Omega + iA_4^\dagger R^\dagger \hat{Q}R + i\gamma_4 \gamma_k A_k^\dagger R^\dagger \hat{Q}R \right] \gamma_4 , \quad (17)$$

where the collective coordinate  $\Omega_M$  is will be quantized according to the canonical quantization rule, which in Minkowski space-time are:

$$\Omega^A \rightarrow \frac{1}{I} \hat{T}^A \equiv \frac{1}{2I} \tau^A . \quad (18)$$

Here  $\hat{T}^A$  are the  $SU(2)$  group generators. The moment of inertia  $I$  has been computed numerically in [13].

Now, using the ansatz (14) the generating functional (4) can be re-expressed in terms of the rotational matrix  $R(t)$  in Euclidean space-time as

$$Z'_{NJL}[A_\mu] = \int \mathcal{D}R(t) \exp [-S_{eff}[A_\mu, R(t), \Omega]] , \quad (19)$$

where  $\Omega$  is a function of  $R \equiv R(t)$  (see eq. (13)). Having the explicit form of the Dirac operator (15) we can go back to the action (5). Since we treat the meson fields classically (*i.e.* at the 0-loop level) the only non-trivial part of the action is the fermionic part (6). By construction (see [5,7]) it is splitted in a natural way into valence and Dirac sea parts. The valence part is finite and it will not be regularized. In this case the calculation is straightforward and the detailed derivation can be found *e.g* in [5]. Hence, from now on we will concentrate on the sea contribution and we will restrict our discussion to that part of the full action.

As we can see from (15), (17), the operator (15) is non-Hermitian. Hence, in general, the action (6) will have the real and imaginary part. To make clear distinction we write down both parts explicitly:

$$S_{eff}^F = \text{Re } S_{eff}^F + \text{Im } S_{eff}^F , \quad (20)$$

$$\text{Re } S_{eff}^F \equiv -\frac{1}{2} \text{ Sp ln}[\tilde{\mathcal{D}}^\dagger \tilde{\mathcal{D}}] , \quad (20a)$$

$$\text{Im } S_{eff}^F \equiv -\frac{1}{2} \text{ Sp ln}[\tilde{\mathcal{D}} / \tilde{\mathcal{D}}^\dagger] , \quad (20b)$$

The imaginary (anomalous) part is finite and does not need regularization. In addition, any regularization of this part of the action would break several important features of the model related to the anomalous structure. On the other hand, the real part is infinite and a regularization is necessary.

In order to compute the nucleon form factors we have to evaluate the expectation value of the electromagnetic current  $j_\mu^{em}$ . To this end we take into account the standard definition given by:

$$\langle j_\mu^{em}(0) \rangle \equiv \frac{1}{Z_0} \left. \frac{\delta Z'_{NJL}[A_\mu]}{\delta A_\mu(0)} \right|_{A_\mu=0} \equiv \frac{1}{Z_0} \int \mathcal{D}R \left. \frac{\delta S_{eff}}{\delta A_\mu(0)} \right|_{A_\mu=0} \exp[-S_{eff}] , \quad (21)$$

where the generating functional  $Z'_{NJL}$  is given by (19).

As it was mentioned above the real part of the action diverges. To calculate the expression (21), we introduce the Schwinger proper-time regularization of the action. In general, for an operator  $\mathcal{A}$  its proper-time regularized form reads [17]:

$$\ln \mathcal{A} = - \lim_{\Lambda \rightarrow \infty} \int_{1/\Lambda^2}^{\infty} \frac{d\tau}{\tau} e^{-\tau \mathcal{A}} . \quad (22)$$

The Schwinger method is especially convenient for the logarithmic expressions resulting from the fermionic determinant. Applying (22) to the action (6) we obtain:

$$S_{eff}^F = \frac{N_c}{2} \sum_n \int d^4x_E \text{Tr}_\gamma \text{Tr}_\tau \int_{\frac{1}{\Lambda^2}}^{\infty} \frac{d\tau}{\tau} \psi_n^\dagger(x_E) \exp[-\tau \tilde{\mathcal{D}}^\dagger \tilde{\mathcal{D}}] \psi_n(x_E) , \quad (23)$$

where  $\psi_n(x)$  is any complete set of eigenfunctions. Actually, in our calculations we shall use for  $\psi_n(x)$  eigenfunctions of the Hamiltonian  $h$ . For the meson fields  $\sigma, \vec{\pi}$  we substitute the static selfconsistent hedgehog solution  $\bar{U}(\vec{x})$  of the chiral soliton [7] form:

$$\sigma(x) = \sigma(r), \quad \vec{\pi}(x) = \hat{r} \pi(r) , \quad (24)$$

restricted to the chiral circle (3). Numerically, we will follow the method of Ripka and Kahana [16] and will use the eigenfunctions of the Hamiltonian  $h$  to compute all matrix elements (see also Section 4).

Now, our task is to evaluate the current (21) with the regularized action (23). The difficulty lies in the fact that the expression (23) contains rather complicated operator exponent in the integrand. However, because afterwards we take derivative over the fields  $A_\mu$  and put  $A_\mu = 0$ , the only nonzero contribution will come from the part of the integrand linear in  $A_\mu$ . We shall treat the cranking parameter  $\Omega \sim \frac{1}{N_c}$  as a small perturbation that is consistent with the large  $N_c$  limit philosophy behind the NJL model. Hence, we can neglect terms  $\Omega^2$  and higher\*. Also, we should be careful in performing the  $\mathcal{DR}$  integration, as in general the operators  $\hat{Q}$  and  $R$  does not commute and one must use the proper time ordering (see Sect. 4 and [18, 19]). In the next step we expand the integrand in (23) in terms of  $A_\mu$  and  $\Omega$ . To this end we apply the Feynman-Schwinger-Dyson (FSD) expansion for the operator exponent:

$$e^{\mathcal{A}+\mathcal{B}} = e^{\mathcal{A}} + \int_0^1 d\alpha e^{\alpha\mathcal{A}} \mathcal{B} e^{(1-\alpha)\mathcal{A}} + \int_0^1 d\beta \int_0^{1-\beta} d\alpha e^{\alpha\mathcal{A}} \mathcal{B} e^{\beta\mathcal{A}} \mathcal{B} e^{(1-\alpha-\beta)\mathcal{A}} + \dots . \quad (25)$$

In our case, for the operator  $\mathcal{A}$  we substitute the part of our operator exponent  $(-\tau W)$ , where:

$$W \equiv \tilde{\mathcal{D}}_E^\dagger \tilde{\mathcal{D}}_E , \quad (26)$$

that does not contain  $A_\mu$  and  $\Omega$ . This part of  $W$  we will call  $W_0$ . On the other hand, for the operator  $\mathcal{B}$  we take the remaining terms of the operator  $W$  and we will call them  $W_1, W_2, \dots, W_5$ . The first type of terms ( $W_1$ ) is defined as the sum of all terms in the exponent that are linear in  $A_\mu$ ,  $W_2 \sim A_\mu \times \Omega$ ,  $W_3 \sim \Omega$ ,  $W_4 \sim \Omega^2$  and  $W_5 \sim A_\mu^2$ . The  $W_5$  contribution to (21) is exactly zero, while the  $W_4$  contribution we neglect as being small (quadratic in  $\Omega$ ). Hence, the operator  $\mathcal{B}$  will include the terms  $W_1-W_3$  only. Finally, this gives us the following expressions for the terms  $W_0-W_3$  of the operator  $W$  (26):

$$W_0 = + \omega^2 + h^2 , \quad (27a)$$

$$\begin{aligned} W_1 = & - (A_4 + A_4^\dagger) R^\dagger \hat{Q} R \omega + (A_k - A_k^\dagger) \gamma_4 \gamma_k R^\dagger \hat{Q} R \omega + \\ & + i (h A_4 R^\dagger \hat{Q} R - A_4^\dagger R^\dagger \hat{Q} R h) - \\ & - (h \gamma_4 \gamma_k A_k R^\dagger \hat{Q} R + \gamma_4 \gamma_k A_k R^\dagger \hat{Q} R h) , \end{aligned} \quad (27b')$$

---

\* Actually, the terms  $\sim \Omega^2$  must be taken into account to evaluate the moment of inertia (see [5, 13] for details).

$$W_2 = - (A_4 \Omega R^\dagger \hat{Q} R + A_4^\dagger R^\dagger \hat{Q} R \Omega) + \gamma_4 \gamma_k (A_k \Omega R^\dagger \hat{Q} R - A_k^\dagger R^\dagger \hat{Q} R \Omega) + \\ + A_4 [\Omega, R^\dagger \hat{Q} R] - \gamma_4 \gamma_k A_k [\Omega, R^\dagger \hat{Q} R], \quad (27c')$$

$$W_3 = + 2 \Omega \omega - i [h, \Omega]. \quad (27d)$$

Taking into account that the electromagnetic potential is Hermitian we get for the  $W_1$  and  $W_2$  the simpler form:

$$W_1 = + i [h, A_4 R^\dagger \hat{Q} R] - i \{h, \gamma_4 \gamma_k A_k R^\dagger \hat{Q} R\} - \\ - 2 A_4 R^\dagger \hat{Q} R \omega, \quad (27b)$$

$$W_2 = - 2 A_4 \Omega R^\dagger \hat{Q} R. \quad (27c)$$

where  $[ , ]$  and  $\{ , \}$  denote commutators and anticommutators, respectively. Also, the sum of all perturbative terms that will contribute the electromagnetic current (21) we will denote by  $V$ :

$$V \equiv W_1 + W_2 + W_3. \quad (28)$$

In addition, the part of  $V$  containing (linear)  $\omega$ -terms will be called  $\omega V_1$  and the  $\omega$ -independent part will be denoted by  $V_0$ . Hence, the full perturbative term reads:

$$V = V_0 \omega^0 + V_1 \omega^1. \quad (28')$$

To obtain (27) we have computed the trace over the Euclidean time in the  $\omega$ -space, the Fourier conjugate to  $x_4$ . To this end we have substituted in (23):

$$\int dx_4 f(\partial_{x_4}) \rightarrow \int \frac{d\omega}{2\pi} f(+i\omega). \quad (29)$$

Also, the formulae (A.4–A.5) from the Appendix have been used.

Applying (27) and (25) we should have in mind that there are, in general, two types of terms in (25): linear and bilinear in  $\mathcal{B}$ . Hence, the products of the terms (27b-27d) can contribute as well. Also, those products should be linear in  $\Omega$  and  $A_\mu$ . This implies that the only  $W$ -term contributing to the second order FSD expansion is of the form:  $W_1 \times W_3$  — the first one linear in the potential  $A_\mu$  and the second one linear in the cranking parameter  $\Omega$ . As we will see later on, those terms will contribute to the electric isovector and magnetic isoscalar parts of the form factors.

As the above considerations were limited to the regularized part of the action a comment concerning the non-regularized parts is in order. In general, there are two types of non-regularized contributions: the valence parts (for all form factors) and the sea parts of both isoscalar form factors. To compute these quantities we can start directly from the non-regularized action (6) as it was done in [5]. The electromagnetic current reads:

$$j_\mu(x) \equiv \frac{S_{eff}[A_\mu]}{\delta A^\mu} \Big|_{A_\mu=0} = N_c \text{Tr}_\gamma \text{Tr}_\tau \sum_n \int \frac{d\omega}{2\pi} \psi_n^\dagger(x) \frac{1}{\omega + ih - \Omega} R^\dagger QR \gamma_4 \gamma_\mu \psi_n(x), \quad (30)$$

where the integral over  $\omega$  stands for the trace in Euclidean time according to (29). Further calculations can be easier done, without using the expansion (25), just expanding (30) in terms of (small)  $\Omega$ . The same results can be obtained by imposing the  $\Lambda^2 \rightarrow \infty$  limit on our regularized expressions (using formulae (A.2) of Appendix).

The second remark concerns our practical calculation of the imaginary part of the action. One can notice that taking reversed Hermicity (anti-Hermitian) electromagnetic potential  $A_\mu$  in (27b', 27c') the imaginary terms are moved to the real part. With this trick and the  $\Lambda^2 \rightarrow \infty$  limit we can calculate all form factors from (27) within our scheme and not referring to the nonregularized action (6).

Now, taking into account (21), (25) and (27-28) we can write down the operator exponent contributing to the electromagnetic current as:

$$\begin{aligned} \int_{-\infty}^{+\infty} \frac{d\omega}{2\pi} \exp[-\tau W] &\simeq -\tau \int_{-\infty}^{+\infty} \frac{d\omega}{2\pi} \sum_n e^{-\tau\omega^2} \langle n | V | n \rangle + \\ &+ \tau^2 \int_{-\infty}^{+\infty} \frac{d\omega}{2\pi} \sum_{m,n} e^{-\tau\omega^2} |\langle n | V | m \rangle|^2 \int_0^1 d\beta \int_0^{1-\beta} d\alpha e^{-\tau(1-\beta)\epsilon_n^2} e^{-\tau\beta\epsilon_m^2}, \end{aligned} \quad (31)$$

where the terms quadratic and higher in  $\Omega$  are neglected and because of the derivative in (21) only the terms linear in potentials are present. To compute the functional (space-time) trace we use the Hamiltonian (8), like for the action (23). Here, the vectors  $|n\rangle$  denotes the eigenfunctions  $\psi_n(x)$  corresponding to the eigenvalues  $\epsilon_n$ .

We cannot perform the  $\omega$ -integrals directly as the operator  $V$  is  $\omega$ -dependent. However, we can simplify (31) taking into account that the term  $|V_{mn}|^2$  is symmetric in indices  $m, n$  and performing trivial  $\alpha$ - and  $\beta$ -integrals. After that the integration over  $\omega$  is performed and we get for the electromagnetic current the following expression:

$$\begin{aligned}
j_{em}^\mu = & \frac{N_c}{4\sqrt{\pi}} \int_{1/\Lambda^2}^\infty \frac{d\tau}{\sqrt{\tau}} \left\{ \sum_n e^{-\tau\epsilon_n^2} \langle n | \frac{\delta V_0}{\delta A_\mu} | n \rangle + \right. \\
& + \sum_{m,n} \frac{e^{-\tau\epsilon_n^2} - e^{-\tau\epsilon_m^2}}{\epsilon_n^2 - \epsilon_m^2} \left[ \langle n | V_0[A_\mu = 0] | m \rangle \langle m | \frac{\delta V_0}{\delta A_\mu} | n \rangle + \right. \\
& \left. \left. + \frac{1}{2\tau} \langle n | V_1[A_\mu = 0] | m \rangle \langle m | \frac{\delta V_1}{\delta A_\mu} | n \rangle \right] \right\}, \tag{32}
\end{aligned}$$

where the notation  $V_1[A_\mu = 0]$  means the sum of all terms linear in  $\omega$  which do not contain  $A_\mu$ . The formula (32) together with (27) will be used in the next Section to obtain the electromagnetic form factors' formulae.

### 3. Computing the form factors

In this point, applying the FSD expansion (25) we are ready to compute the electromagnetic form factors directly from the regularized action (23) which includes the fermion loop corrections. The nucleon electromagnetic Sachs form factors are defined by:

$$\langle N(p) | j_0^{em}(0) | N(p') \rangle = G_E(q^2), \tag{33a}$$

$$\langle N(p) | j_i^{em}(0) | N(p') \rangle = \frac{1}{2\mathcal{M}_N} G_M(q^2) i \epsilon_{ikl} q^k \langle N | \sigma^l | N \rangle, \tag{33b}$$

where  $|N(p')\rangle$  is the nucleon state with proper spin and isospin quantum numbers. The electromagnetic current  $j_\mu^{em}(x)$  is in the Minkowski space-time and  $\mathcal{M}_N$  is the nucleon mass. It is clear from (33) that to compute the electromagnetic form factors we need the current evaluated in the previous Section. The isoscalar and isovector parts of the form factors are defined by:

$$G_{E,M} \equiv \frac{1}{2} G_{E,M}^{T=0} + \hat{T}_3 G_{E,M}^{T=1}. \tag{34}$$

The Sachs form factors (33) are appropriate for the non-relativistic limit ( $\vec{q}^2 \ll \mathcal{M}_N$ ) that is consistent with the large  $N_c$  approximation.

The isoscalar form factors (electric and magnetic) come from the scalar part of the quark current matrix  $\hat{Q}$  ( $\sim \hat{1}$ ) while the isovector form factors is from the triplet part ( $\sim \tau^3$ ). The terms linear in  $\Omega$  contribute to the electric isovector and to both magnetic form factors. As

can be easily checked directly from (27) and (32), the contribution from the real part of the action to both the isoscalar electric form factor and the isoscalar magnetic one is exactly zero. This means that these form factors originate from the imaginary part of the action and they will not be regularized. Table 1 lists terms contributing to a given form factor. In the last column we explicitly indicate which form factor should be regularized.

Table 1. Terms of the effective action contributing to different electromagnetic form factors.

| quantity    | $A_\mu$ | $\Omega$              | $\hat{Q}$      | 2 <sup>0</sup> -order FSD | $V_\omega$ | regularized |
|-------------|---------|-----------------------|----------------|---------------------------|------------|-------------|
| $G_E^{T=0}$ | $A_4$   | $\Omega^0$            | $\sim \hat{1}$ | NO                        | NO         | NO          |
| $G_E^{T=1}$ | $A_4$   | $\Omega^1$            | $\sim \tau^3$  | YES                       | YES        | YES         |
| $G_M^{T=0}$ | $A_k$   | $\Omega^1$            | $\sim \hat{1}$ | YES                       | NO         | NO          |
| $G_M^{T=1}$ | $A_k$   | $\Omega^0 + \Omega^1$ | $\sim \tau^3$  | NO + YES                  | NO         | YES + NO    |

The electric scalar form factor can be immediately extracted from (33a) and (30). Since only the isoscalar part of the operator  $\hat{Q}$  contributes the rotational matrices  $R(t)$  vanish from the action. Hence, the  $D\mathcal{R}$  integration in (19) becomes trivial. Also, in this case the contribution from the terms linear in  $\Omega$  is exactly equal to zero. Finally we arrive at:

$$G_E^{T=0}(q^2) = \int d^3x e^{-i\vec{q}\vec{x}} \frac{N_c}{3} \left\{ \sum_{n \in VAL} \psi_n^\dagger(\vec{x}) \psi_n(\vec{x}) - \sum_{n \in ALL} \frac{1}{2} \text{sign}(\epsilon_n) \psi_n^\dagger(\vec{x}) \psi_n(\vec{x}) \right\}, \quad (35)$$

where **VAL** denotes the valence whereas **ALL** stands for all eigenstates of the Hamiltonian including the valence one as well. The first term in eq.(35) comes from the valence quarks and the second term is due to the quark vacuum polarization. As has been stated previously, the same result can be obtained by substituting anti-Hermitian fields  $A_\mu$  in (27b'), using (32), and taking the limit  $\Lambda^2 \rightarrow \infty$ .

As the next step, we compute the electric isovector form factor. In this case, the regularization is necessary and the second order terms in the FSD expansion have to be taken into account. Contribution to the first order come from the terms of  $W_2$  containing both  $A_4$  and  $\Omega$ . The second order includes terms from  $W_1$  and  $W_3$ .

In the first order FSD term we insert unity:  $\sum_m \psi_m^\dagger(x) \psi_m(x)$  and we get identical overall isospin-space factor of the form:

$$j_4^{em} \sim \psi_n^\dagger \Omega \psi_m \psi_m^\dagger R \tau^3 R^\dagger \psi_n , \quad (36)$$

to which the Fierz identity (A.6) is applied. Then, we express  $\Omega$  in terms of the rotational matrix  $R$  using the identity:

$$\Omega \equiv -iR\dot{R}^\dagger \equiv -i\dot{R}^\dagger R \quad (37)$$

and (A.7).

Finally, from the quantization rule for the collective coordinate  $\Omega$  (18), where the moment of inertia  $I$  has been computed numerically in [13], we arrive at the following expression for the electric isovector form factor:

$$\begin{aligned} G_E^{T=1}(q^2) = & \int d^3x e^{-iq\vec{x}} \frac{-N_c}{6I} \int d^3y \left\{ \sum_{\substack{n \in VAL \\ m \in ALL}} \frac{\psi_n^\dagger(\vec{x}) \tau^A \psi_m(\vec{x}) \psi_m^\dagger(\vec{y}) \tau^A \psi_n(\vec{y})}{\epsilon_n - \epsilon_m} + \right. \\ & + \frac{1}{4\sqrt{\pi}} \sum_{m,n \in ALL} \int_{\frac{1}{\Lambda^2}}^{\infty} \frac{d\tau}{\sqrt{\tau}} \left[ \frac{\epsilon_n e^{-\tau\epsilon_n^2} + \epsilon_m e^{-\tau\epsilon_m^2}}{\epsilon_n + \epsilon_m} + \frac{1}{\tau} \frac{e^{-\tau\epsilon_n^2} - e^{-\tau\epsilon_m^2}}{\epsilon_n^2 - \epsilon_m^2} \right] \times \quad (38) \\ & \left. \times \psi_n^\dagger(\vec{x}) \tau^A \psi_m(\vec{x}) \psi_m^\dagger(\vec{y}) \tau^A \psi_n(\vec{y}) \right\}, \end{aligned}$$

The formula (38) for  $q^2 = 0$  is equivalent to the quotient of the moment of inertia by itself and:  $G_E^{T=1}(q^2 = 0) = 1$ , as it should be.

We proceed to compute the magnetic form factors. We start with the isoscalar one. In this case, the contribution comes from the imaginary part of the action and the regularization is not necessary. The quark current matrix  $\hat{Q}$  contributes *via* the isoscalar term,  $\sim \frac{1}{6} \hat{1}$ , diagonal in the isospin space. Hence, the rotation matrices  $R(t)$  cancel each other and, like for the electric scalar form factor, there is no time ordering problem for the  $\mathcal{D}R$  integration in (19). However, there is still a nonzero contribution from terms linear in  $\Omega$ . Starting from the reversed Hermicity of  $A_\mu$  and the regularized (real) action term (27c') we find that contribution to the first order FSD expansion comes from the anticommutator term:  $\gamma_4 \gamma_k A_k \{\Omega, R\hat{Q}R^\dagger\} = \frac{1}{3} \gamma_4 \gamma_k A_k \Omega$ . It contributes to the electromagnetic current as follows:

$$j_{em}^k(1) = \frac{N_c}{12\sqrt{\pi}} \int_{\frac{1}{\Lambda^2}}^{\infty} \frac{d\tau}{\sqrt{\tau}} \sum_n e^{-\tau\epsilon_n^2} \langle n | \gamma_4 \gamma_k \Omega | n \rangle . \quad (39)$$

The second order FSD contribution comes from the terms  $\frac{1}{3}A_k\gamma_4\gamma_k\omega - \frac{i}{6}[h, \gamma_4\gamma_kA_k]$  (in  $W_1$ ) and  $2\Omega\omega - i[h, \Omega]$  (in  $W_3$ ). Taking into account (32) and (39) together with (13) and (18) we obtain the space components of the isoscalar electromagnetic current in Euclidean space-time in the following form:

$$j_k^{em} = \frac{-N_c}{48\sqrt{\pi}I} \int_{\frac{1}{\Lambda^2}}^{\infty} \frac{d\tau}{\sqrt{\tau}} \sum_{m,n} \left[ \frac{\epsilon_n e^{-\tau\epsilon_n^2} + \epsilon_m e^{-\tau\epsilon_m^2}}{\epsilon_n + \epsilon_m} + \frac{1}{\tau} \frac{e^{-\tau\epsilon_n^2} - e^{-\tau\epsilon_m^2}}{\epsilon_n^2 - \epsilon_m^2} \right] \times \quad (40)$$

$$\times \int d^3y \langle N | \tau^A | N \rangle \psi_n^\dagger(\vec{x}) \gamma_4 \gamma_k \psi_m(\vec{x}) \psi_m^\dagger(\vec{y}) \tau^A \psi_n(\vec{y}) .$$

Now, we have to perform transformation to the Minkowski space-time. Also, one has once again to resolve (33b), this time with respect to the form factor  $G_M^{T=0}$ . To this end we apply (A.9) and the result for the sea part of the magnetic isoscalar form factor reads:

$$G_M^{T=0}(q^2) \Big|_{sea} = \int d^3x e^{-iq\vec{x}} \frac{-N_c \mathcal{M}_N}{24\sqrt{\pi}I} \int d^3y \epsilon_{ijA} \frac{q_j}{q^2} \times \quad (41)$$

$$\times \sum_{m,n \in ALL} \int_{\frac{1}{\Lambda^2}}^{\infty} \frac{d\tau}{\sqrt{\tau}} \left[ \frac{\epsilon_n e^{-\tau\epsilon_n^2} + \epsilon_m e^{-\tau\epsilon_m^2}}{\epsilon_n + \epsilon_m} + \frac{1}{\tau} \frac{e^{-\tau\epsilon_n^2} - e^{-\tau\epsilon_m^2}}{\epsilon_n^2 - \epsilon_m^2} \right] \times$$

$$\times \psi_n^\dagger(\vec{x}) \gamma_0 \gamma_i \psi_m(\vec{x}) \psi_m^\dagger(\vec{y}) \tau^A \psi_n(\vec{y}) .$$

To obtain the full form factor we must add to (41) the valence contribution and we must take the non-regularized limit:  $\Lambda^2 \rightarrow \infty$ . For the last step we use formulae (A.2) to find that:

$$\lim_{\Lambda^2 \rightarrow \infty} \int_{1/\Lambda^2}^{\infty} \frac{d\tau}{\sqrt{\tau}} \left[ \frac{\epsilon_n e^{-\tau\epsilon_n^2} + \epsilon_m e^{-\tau\epsilon_m^2}}{\epsilon_n + \epsilon_m} + \frac{1}{\tau} \frac{e^{-\tau\epsilon_n^2} - e^{-\tau\epsilon_m^2}}{\epsilon_n^2 - \epsilon_m^2} \right] = \quad (42)$$

$$= \frac{-\sqrt{\pi}}{\epsilon_n - \epsilon_m} [\text{sign}(\epsilon_n) - \text{sign}(\epsilon_m)] .$$

Finally, we get for the magnetic isoscalar form factor the following expression:

$$\begin{aligned}
G_M^{T=0}(q^2) = & \int d^3x e^{-i\vec{q}\vec{x}} \frac{N_c \mathcal{M}_N}{6I} \int d^3y \epsilon_{ijA} \frac{q_j}{q^2} \times \\
& \times \left\{ \sum_{\substack{n \in VAL \\ m \in ALL}} \frac{\psi_n^\dagger(\vec{x}) \gamma_0 \gamma_i \psi_m(\vec{x}) \psi_m^\dagger(\vec{y}) \tau^A \psi_n(\vec{y})}{\epsilon_n - \epsilon_m} \right. \\
& \left. + \frac{1}{2} \sum_{\substack{n \in VAL \\ m \in ALL}} \text{sign}(\epsilon_n) \frac{\psi_n^\dagger(\vec{x}) \gamma_0 \gamma_i \psi_m(\vec{x}) \psi_m^\dagger(\vec{y}) \tau^A \psi_n(\vec{y})}{\epsilon_n - \epsilon_m} \right\}, \tag{43}
\end{aligned}$$

where, as usually, summation over repeated indices  $i, j, A$  is assumed. The first part gives the valence and the second part the sea contribution to the form factor.

For the magnetic isovector form factor the sea contribution comes from the isotriplet part of the quark current matrix  $\hat{Q}$ . Because of this we cannot get rid of the rotation matrix  $R(t)$  in the action.

First, let us compute contribution from the first order FSD expansion (0-order in  $\Omega$ ). This term is the anticommutator  $-\frac{i}{2}\{h, \gamma_4 \gamma_k A_k R \tau^3 R^\dagger\}$  in (27b). This implies for the electromagnetic current:

$$j_k^{em} = \frac{i N_c}{4\sqrt{\pi}} \sum_n \int_{\frac{1}{\Lambda^2}}^{\infty} \frac{d\tau}{\sqrt{\tau}} \epsilon_n e^{-\tau \epsilon_n^2} \langle n | \gamma_4 \gamma_k \tau^3 | n \rangle, \tag{44a}$$

where we are still in the Euclidean space-time. Taking into account (A.8) and  $\gamma_0$  instead of  $\gamma_4$  we get:

$$j_k^{em} = \frac{-N_c}{8\sqrt{\pi}} \text{Tr}(R \tau^3 R^\dagger \tau^A) \sum_n \int_{\frac{1}{\Lambda^2}}^{\infty} \frac{d\tau}{\sqrt{\tau}} \epsilon_n e^{-\tau \epsilon_n^2} \langle n | \gamma_0 \gamma_k \tau^A | n \rangle, \tag{44b}$$

For the term (44b) regularization is necessary, as it comes from the real part of the action and is infinite.

For the linear order in  $\Omega$  we have to take into account non-commutativity of the isospin operator in the collective variable (18) with the finite rotation (Wigner) matrix. This leads to the extra term, linear in the cranking parameter. The observation has been done in [18] in the context of the axial coupling constant  $g_A$ , and the proper treatment of such effect for the  $g_A$  and the isovector magnetic moment has been given in [19].

Following the method of [19] we get the additional, linear in  $\Omega$  correction to the isovector electromagnetic current in the form:

$$j_k^{iem\ A}(\Omega^1) = N_c [\Omega_C, \frac{1}{2}\text{Tr}(R^\dagger \tau^A R \tau^B)] \sum_{\substack{m \in VAL \\ n \in ALL}} \int d^3y \frac{\psi_n^\dagger(\vec{x}) \gamma_0 \gamma_k \tau^B \psi_m(\vec{x}) \psi_m^\dagger(\vec{y}) \tau^C \psi_n(\vec{y})}{\epsilon_n - \epsilon_m}. \quad (45)$$

Here, a remark concerning regularization of the term (45) is in order. This expression is numerically finite and, as has been shown in [19], it is finite in the gradient expansion. Hence, the regularization is not necessary. Also, one should have in mind that the main contribution to the isovector magnetic current comes from the valence part, the sea contribution is relatively small and the formal regularization of that contribution gives a small difference with our result.

To calculate the form factor we have to resolve the equation (33b) with respect to  $G_M^{T=1}$  using the spherical basis in which the rotation matrices  $R(t)$  are related to the Wigner functions. Our current (44b) has the general index structure of the form:  $j_k = X^A \epsilon_{kAi} q_i F(q)$ . Comparing this structure with eqs. (33b,34), using (A.9) we obtain the final expression for the magnetic isovector form factor in the following form:

$$\begin{aligned} G_M^{T=1}(q^2) = & \int d^3x e^{-iq\vec{x}} \frac{iN_c \mathcal{M}_N}{3} \epsilon_{ijA} \frac{q_j}{q^2} \left\{ \sum_{n \in VAL} \psi_n^\dagger(\vec{x}) \gamma_0 \gamma_i \tau^A \psi_n(\vec{x}) - \right. \\ & - \frac{1}{2\sqrt{\pi}} \sum_{n \in ALL} \int_{\frac{1}{\Lambda^2}}^{\infty} \frac{d\tau}{\sqrt{\tau}} \epsilon_n e^{-\tau \epsilon_n^2} \psi_n^\dagger(\vec{x}) \gamma_0 \gamma_i \tau^A \psi_n(\vec{x}) + \\ & \left. + \frac{1}{6I} \epsilon_{ABC} \sum_{\substack{n > val \\ m \leq val}} \int d^3y \frac{\psi_n^\dagger(\vec{x}) \gamma_0 \gamma_i \tau^B \psi_m(\vec{x}) \psi_m^\dagger(\vec{y}) \tau^C \psi_n(\vec{y})}{\epsilon_n - \epsilon_m} \right\}. \end{aligned} \quad (46)$$

The proton and neutron form factors are defined, respectively, as sum and difference of the isoscalar and isovector form factors:

$$G_{E,M}^p = \frac{1}{2} [G_{E,M}^{T=0} + G_{E,M}^{T=1}], \quad (47a)$$

$$G_{E,M}^n = \frac{1}{2} [G_{E,M}^{T=0} - G_{E,M}^{T=1}], \quad (47b)$$

and the numerical results for them are presented in Section 4.

#### 4. Numerical results

To compute observables we use the finite quasi-discrete basis and numerical method of Ripka and Kahana [16] for solving the eigenvalue problem. The Hamiltonian  $h$  is taken in a spherical box of a large radius  $D$ . The basis is made discrete by imposing a boundary condition at  $r = D$ . Also, it is made finite by restricting momenta of the basis states to be smaller than the numerical cut-off  $K_{max}$ . Both quantities have no physical meaning and the results should not depend on them. The typical values used are  $D \sim 20/M$  and  $K_{max} \sim 7M$ .

In addition, all checks concerning the numerical stability of the solution with respect to varying box size and choice of the numerical cut-off have been done and the actual calculation is completely under control.

The actual calculations are done by fixing the parameters in meson sector in the well known way [7] to have  $f_\pi = 93\text{ MeV}$  and  $m_\pi = 139.6\text{ MeV}$ . This leaves the constituent quark mass  $M$  as the only free parameter.

The proton and neutron electric and magnetic form factors are displayed in figs.1–4. The theoretical curves resulting from the model are given for the following four values the constituent quark mass: 370, 400, 420 and 450 MeV. The magnetic form factors are normalized to the experimental values of the corresponding magnetic moments at  $q^2 = 0$ . With one exception of the neutron electric form factor (fig. 2), all other form factors fit to the experimental data quite well. The best fit is for the constituent quark mass around 400–420 MeV.

As can be seen the only form factor which deviates from the experimental data is the neutron electric form factor and this requires some explanation. Obviously, this form factor is the most sensitive for numerical errors. According to the formula (47b) the form factor has been calculated as a difference of the electric isoscalar and electric isovector form factors that were the direct output of our code. Both form factors were of order 1.00 and calculated by the code with rather high accuracy of about 1%. However, the resulting neutron form factor has the proper (experimental) value of order 0.04, *i.e.* about 4% of the value of its components. This means that a small numerical error for one of the components can be enhanced by a factor 50. Hence, small numerical errors together with the applied approximations (like the  $1/N_c$  approximation behind the model and neglecting the boson-loop effects as well as higher order fermion loops) are strongly magnified resulting in a considerable deviation from the experimental data for momentum transfers above  $100\text{ MeV}/c$ .

As the next step, one can compute other electromagnetic observables: the mean squared radii, the magnetic moments and the nucleon– $\Delta$  splitting. The static nucleon properties, in particular the charge radii and the magnetic moments can be obtained from the form factors:

$$\langle r^2 \rangle_{T=0,1} = -\frac{dG_E^{T=0,1}}{dq^2} \left. \frac{6}{G_E^{T=0,1}} \right|_{q^2=0}, \quad (48)$$

$$\mu^{T=0,1} = G_M^{T=0,1}(q^2) \Big|_{q^2=0}. \quad (49)$$

For the quark masses 370, 420 and 450 MeV and pion mass  $m_\pi = 140\text{MeV}$  the calculated values are presented in table 2. For comparison, in table 3 we give the theoretical values for the same quantities but with the physical pion mass set to zero.

Table 2. Nucleon observables computed with the physical pion mass.

| Quantity                                  | Constituent Quark Mass |       |         |       |         |       | Exper. |
|---|------------------------|-------|---------|-------|---------|-------|--------|
|   | 370 MeV                |       | 420 MeV |       | 450 MeV |       |        |
|   | total                  | sea   | total   | sea   | total   | sea   |        |
| $\langle r^2 \rangle_{T=0} [\text{fm}^2]$ | 0.63                   | 0.05  | 0.52    | 0.07  | 0.48    | 0.09  | 0.62   |
| $\langle r^2 \rangle_{T=1} [\text{fm}^2]$ | 1.07                   | 0.33  | 0.89    | 0.41  | 0.84    | 0.45  | 0.86   |
| $\langle r^2 \rangle_p [\text{fm}^2]$     | 0.85                   | 0.19  | 0.70    | 0.24  | 0.66    | 0.27  | 0.74   |
| $\langle r^2 \rangle_n [\text{fm}^2]$     | -0.22                  | -0.14 | -0.18   | -0.17 | -0.18   | -0.18 | -0.12  |
| $\mu_{T=0} [\text{n.m.}]$                 | 0.68                   | 0.09  | 0.62    | 0.03  | 0.59    | 0.05  | 0.88   |
| $\mu_{T=1} [\text{n.m.}]$                 | 3.74                   | 0.96  | 3.53    | 1.07  | 3.47    | 1.17  | 4.71   |
| $\mu_p [\text{n.m.}]$                     | 2.21                   | 0.53  | 2.08    | 0.55  | 2.03    | 0.61  | 2.79   |
| $\mu_n [\text{n.m.}]$                     | -1.53                  | -0.44 | -1.46   | -0.52 | -1.44   | -0.56 | -1.91  |
| $ \mu_p/\mu_n $                           | 1.44                   | —     | 1.42    | —     | 1.41    | —     | 1.46   |
| $M_\Delta - M_N [\text{MeV}]$             | 213                    | —     | 280     | —     | 314     | —     | 294    |
| $g_A$                                     | 1.32                   | 0.15  | 1.29    | 0.20  | 1.29    | 0.23  | 1.26   |

The chiral limit  $m_\pi \rightarrow 0$  mostly influences the isovector charge radius. In fact, as illustrated in fig.5, where the isovector charge radius is plotted *vs.* the box size  $D$ , it grows linearly with  $D$  and diverges as  $D \rightarrow \infty$ . Because of this that quantity (and the derivative quantities) are not included in table 3. The other quantity strongly influenced by the chiral limit is the neutron electric form factor. For the  $m_\pi \rightarrow 0$  the discrepancy from the experiment is larger by almost a factor two than in the case  $m_\pi \neq 0$ . The other quantities differ in the chiral limit by about 30%. The comparison of values in the two tables indicate that taking the physical pion mass gives us a best fit with a much better agreement

with the experimental data. To be particular, in the calculations with zero pion mass the electric observables suggest a high value ( $M \sim 450 \text{ MeV}$ ) while the magnetic ones indicate  $M \sim 370 \text{ MeV}$  which is not the case with physical pion mass. In addition, we observe much larger contribution from the sea effects, about 50% of the total value.

Table 3. Nucleon observables computed with the zero pion mass.

| Quantity                                  | Constituent Quark Mass |       |         |       |         |       | Exper. |
|---|------------------------|-------|---------|-------|---------|-------|--------|
|   | 370 MeV                |       | 420 MeV |       | 450 MeV |       |        |
|   | total                  | sea   | total   | sea   | total   | sea   |        |
| $\langle r^2 \rangle_{T=0} [\text{fm}^2]$ | 0.88                   | 0.20  | 0.66    | 0.26  | 0.61    | 0.23  | 0.62   |
| $\mu_{T=0} [\text{n.m.}]$                 | 0.66                   | 0.07  | 0.59    | 0.09  | 0.57    | 0.09  | 0.88   |
| $\mu_{T=1} [\text{n.m.}]$                 | 4.84                   | 1.98  | 4.50    | 2.09  | 4.29    | 2.16  | 4.71   |
| $\mu_p [\text{n.m.}]$                     | 2.75                   | 1.03  | 2.54    | 1.09  | 2.43    | 1.13  | 2.79   |
| $\mu_n [\text{n.m.}]$                     | -2.09                  | -0.96 | -1.95   | -1.00 | -1.86   | -1.03 | -1.91  |
| $ \mu_p/\mu_n $                           | 1.31                   | —     | 1.30    | —     | 1.31    | —     | 1.46   |
| $M_\Delta - M_N [\text{MeV}]$             | 221                    | —     | 261     | —     | 301     | —     | 294    |
| $g_A [\text{MeV}]$                        | 1.34                   | 0.24  | 1.29    | 0.15  | 1.25    | 0.00  | 1.26   |

The results of table 2 ( $m_\pi = 140 \text{ MeV}$ ) again indicate the value  $\sim 400\text{--}420 \text{ MeV}$  for the constituent quark mass, in agreement with the conclusion drawn from the form factor curves. The same has been suggested earlier [13–15], where smaller number of observables has been taken into account. With the exception of the neutron electric squared radii, to which remarks similar to the case of the neutron electric form factor are applicable, the contribution of the valence quarks is dominant. However, the contribution of the Dirac sea is non-negligible, it lies within the range 15 – 40%.

One can notice, that the numerical results for the nucleon– $\Delta$  mass splitting ( $M_\Delta - M_N$ ), the mean squared proton, isoscalar and isovector electric radii and the axial coupling constant ( $g_A$ ), as well as the proton electric and magnetic and neutron magnetic form factor, differ from the experimental data by no more than about  $\pm 5\%$ . Finally, for the magnetic moments we have got results 20–25% below their experimental values. Despite of this underestimation of both magnetic moments we have found surprisingly good result for the ratio  $\mu_p/\mu_n$  which is far better than in other models. The agreement with the experimental value is better than 3% for the constituent quark mass 420 MeV. So good result has been obtained neither in

the Skyrme, nor in the linear chiral model.

The isoscalar and isovector electric mean squared radii are shown in figs. 6–7 as functions of the constituent quark mass. The same plot but for the experimentally measured quantities: the proton and neutron electric charge radii, is given in fig. 8. In these plots the valence and sea contributions are explicitly given (dashed and dash-dotted lines, respectively). As could be expected, for the isoscalar electric charge radius the valence part is dominant (about 85%), due to the fact that there is no contribution from the terms linear in the collective coordinate  $\Omega$ . This is not true for the isovector electric charge radius, where the sea part contributes to about 45% of the total value (fig. 7). Also, this effect can be seen from the proton and neutron charge radii (fig. 8) which are linear combinations of the isoscalar and isovector ones. For proton the sea contribution is about 30%. However, for the neutron charge radius the sea part is dominating and the valence contribution is negligible.

In addition, in fig. 9 we plot the magnetic moment density distribution for proton and neutron for the constituent quark mass  $M = 420 \text{ MeV}$ . The sea contribution becomes non-negligible for distances greater than  $0.5 \text{ fm}$ . Due to the relatively large tail contribution to the magnetic moments the sea contribution to these quantities is about 30%. If one is interested in the proton and neutron charge distribution the reader is referred to ref. [15].

Both the magnetic moments and the electric radii are rather sensitive to the tail behaviour of the corresponding densities. In actual calculations of these quantities the densities are integrated with extra factors  $r$  for the magnetic moments and  $r^2$  for the radii that enhances the role of the tail. This leads to the strong enhancement of numerical errors and partially it explains the deviations.

## 5. Summary and conclusions

Our numerical results support the view that chiral quark soliton model of the Nambu–Jona-Lasinio type offers relatively simple but quite successful description of some low-energy QCD phenomena and, in particular, of the electromagnetic properties of nucleons. For the first time the magnetic form factors are calculated. We have obtained quite good results for the electromagnetic form factors, the mean squared radii, the magnetic moments and the nucleon– $\Delta$  splitting reported in figs. 1–4 and tables 2, 3.

Using  $f_\pi = 93 \text{ MeV}$  and  $m_\pi = 139.6 \text{ MeV}$  and a constituent quark mass of  $M = 420 \text{ MeV}$  the isoscalar and isovector electric radii are reproduced within 15%. The magnetic moments are underestimated by about 25%, however, their ratio  $\mu_p/\mu_n$  is almost perfectly

reproduced. The  $q$ -dependence of  $G_E^p(q^2)$ ,  $G_M^p(q^2)$  and  $G_M^n(q^2)$  is very well reproduced. The neutron form factor  $G_E^n(q^2)$  is by a factor of two too large for  $q^2 > 100 \text{ MeV}^2$ . One should note, however, that  $G_E^n(q^2)$  is more than an order of magnitude smaller than  $G_E^p(q^2)$  and as such it is extremely sensitive to both the model approximations and the numerical techniques used. Altogether it is fair to say that the NJL in  $SU(2)$  reproduces reasonably well the electromagnetic properties of the nucleon. Here, it turns out that the agreement is noticeably worse if the chiral limit,  $m_\pi \rightarrow 0$ , is used. This can easily be understood since the pion mass determines the asymptotic behaviour of the pion field. Altogether we conclude that the bosonized NJL model chiral quark soliton model based on a bosonized NJL type lagrangean is quite appropriate for the evaluation of nucleonic electromagnetic properties.

### Acknowledgement:

*We would like to thank Victor Petrov and Pavel Pobylitsa for numerous helpful discussions. The project has been partially supported by the BMFT, DFG and COSY (Jülich). Also, we are greatly indebted for financial support to the Bulgarian Science Foundation Φ-32 (CVC) and to the Polish Committee for Scientific Research, Projects KBN nr 2 P302 157 04 and 2 0091 91 01 (AZG).*

### References

- [1] T.H.Skyrme *Nucl.Phys.* **31** (1962) 556.
- [2] J.Nambu, G.Jona-Lasinio, *Phys.Rev.* **122** (1961) 345.
- [3] T.Eguchi, H.Sugawara, *Phys.Rev.* **D10** (1974) 4257; T.Eguchi, *Phys.Rev.* **D14** (1976) 2755.
- [4] D.Dyakonov, V.Petrov, *Phys.Lett.* **147B** (1984) 351; *Nucl.Phys.* **B272** (1986) 457.
- [5] D.Dyakonov, V.Petrov, P.Pobylitsa, *Nucl.Phys.* **B306** (1988) 809.
- [6] H.Reinhardt, R.Wünsch, *Phys.Lett.* **215B** (1989) 825.
- [7] Th.Meissner, K.Goeke, F.Grümmer, *Phys.Lett.* **227B** (1989) 296; *Ann.Phys.* **202** (1990) 297.
- [8] D.Ebert, M.K.Volkov, *Z.Phys.* **C16** (1983) 205.
- [9] V.Bernard *et al* *Nucl.Phys.* **A412** (1984) 349.
- [10] Th.Meissner, K.Goeke, *Nucl.Phys.* **A524** (1991) 719.
- [11] R.Ball, *Phys.Rep.* **182** (1989) 1.
- [12] M.Schaden, H.Reinhardt, P.Amundsen, M.Lavelle, *Nucl.Phys.* **B339** (1990) 595.

- [13] K.Goeke, A.Z.Górski, F.Grümmer, Th.Meissner, H.Reinhardt, R.Wünsch, *Phys.Lett.* **B256** (1991) 321.
- [14] M.Wakamatsu, H.Yoshiki, *Nucl.Phys.* **A524** (1991) 561.
- [15] A.Z.Górski, K.Goeke, F.Grümmer, *Phys.Lett.* **B278** (1992) 24.
- [16] S.Kahana, G.Ripka, *Nucl.Phys.* **A419** (1984) 462.
- [17] J.Schwinger, *Phys.Rev.* **82** (1951) 664.
- [18] M.Wakamatsu, T.Watabe, *Phys.Lett.* **B312** (1993) 184.
- [19] Ch.Christov, K.Goeke, V.Yu.Petrov, P.V.Pobylitsa, M.Wakamatsu, T.Watabe, preprint RUB-TPII-53/93, Nov 1993 (submitted to: *Phys.Lett.* **B**).

## Appendix

In Euclidean space we use the metric tensor's signature transformed from  $(+ - - -)$  to  $(- - - -)$  (*i.e.* the Euclidean metric tensor  $g_{\mu\nu}^E \equiv -\delta_{\mu\nu}$ ) and the general formulae to perform the transformation from Minkowski to Euclidean space are:

$$\begin{aligned} a_4^E &= +ia_0^M, & a_4^4 &= -ia_M^0, & a_k^E &= +a_k^M, \\ \gamma_4^E &= +i\gamma_0^M, & \gamma_k^E &= +\gamma_k^M, \\ \{\gamma_\mu^E, \gamma_\nu^E\} &= -2\delta_{\mu\nu}, & \{\gamma_\mu^E, \gamma_5^E\} &= 0, \\ (\gamma_\mu^E)^\dagger &= -\gamma_\mu^E, & (\gamma_5^E)^\dagger &= +\gamma_5^E = \gamma_5^M. \end{aligned} \tag{A.1}$$

Here, the simple substitution rule for the limits of basic  $\tau$ -integrals are given to calculate the non-regularized formulae for observables:

$$\lim_{\Lambda^2 \rightarrow \infty} \int_{1/\Lambda^2}^{\infty} \frac{d\tau}{\tau^{1/2}} \alpha e^{-\tau\alpha^2} \rightarrow \sqrt{\pi} \operatorname{sign}(\alpha), \tag{A.2a}$$

$$\lim_{\Lambda^2 \rightarrow \infty} \int_{1/\Lambda^2}^{\infty} \frac{d\tau}{\tau^{3/2}} e^{-\tau\alpha^2} \rightarrow -2\pi |\alpha|, \tag{A.2b}$$

where  $\alpha$  is a real number. In addition, we can express the  $\operatorname{sign}(x)$  function in terms of the step function as:

$$\operatorname{sign}(x) \equiv \Theta(x) - \Theta(-x) \equiv 1 - 2\Theta(-x). \tag{A.3}$$

To obtain the formulae (27) we have applied simple identity for the time derivative of the operator  $R\hat{Q}R^\dagger$ , implied by (13):

$$\partial_4(R\hat{Q}R^\dagger) = i[R\hat{Q}R^\dagger, \Omega]. \tag{A.4}$$

Also, one should have in mind that our potentials  $A_\mu(x)$  are time-independent and we can use identity:

$$\partial_4 A_4 \equiv \partial_4 A_k \equiv 0. \tag{A.5}$$

For the second order FSD expansion it is useful to apply the Fierz identity. If the matrices  $\hat{A}, \hat{B}$ :  $\hat{A} \equiv \frac{1}{2}A^A\tau^A$ ,  $\hat{B} \equiv \frac{1}{2}B^A\tau^A$ , then we get:

$$\operatorname{Tr}(\hat{A}\tau^A) \operatorname{Tr}(\hat{B}\tau^A) = 2 \operatorname{Tr}(\hat{A}\hat{B}). \tag{A.6'}$$

This can be applied to our overall isospin factor in the electromagnetic current as follows:

$$\begin{aligned}
& \sum_{m,n} \int d\Omega_{\vec{x}} d\Omega_{\vec{y}} \psi_n^\dagger(\vec{y}) \Omega \psi_m(\vec{y}) \psi_m^\dagger(\vec{x}) R^\dagger \tau^3 R \psi_n(\vec{x}) = \\
& \sum_{m,n} \frac{1}{4} \text{Tr}(\Omega \tau^A) \text{Tr}(R^\dagger \tau^3 R \tau^B) \int d\Omega_{\vec{x}} d\Omega_{\vec{y}} \psi_n^\dagger(\vec{y}) \tau^A \psi_m(\vec{y}) \psi_m^\dagger(\vec{x}) \tau^B \psi_n(\vec{x}) = \\
& \sum_{m,n} \frac{1}{12} \text{Tr}(\Omega \tau^A) \text{Tr}(R^\dagger \tau^3 R \tau^A) \int d\Omega_{\vec{x}} d\Omega_{\vec{y}} \psi_n^\dagger(\vec{y}) \tau^B \psi_m(\vec{y}) \psi_m^\dagger(\vec{x}) \tau^B \psi_n(\vec{x}) = \\
& \sum_{m,n} \frac{1}{6} \text{Tr}(\Omega R^\dagger \tau^3 R) \int d\Omega_{\vec{x}} d\Omega_{\vec{y}} \psi_n^\dagger(\vec{y}) \tau^A \psi_m(\vec{y}) \psi_m^\dagger(\vec{x}) \tau^A \psi_n(\vec{x}) .
\end{aligned} \tag{A.6}$$

Further simplification is done using the identity:

$$\text{Tr}(\Omega R \tau^3 R^\dagger) = -i \text{Tr}(R \dot{R}^\dagger R \tau^3 R^\dagger) = -i \text{Tr}(\dot{R}^\dagger R \tau^3) = \Omega^3 , \tag{A.7}$$

where we have used (37) and the obvious identity:

$$\hat{A} \equiv \frac{1}{2} \text{Tr}(\hat{A} \tau^A) \tau^A . \tag{A.8}$$

To resolve the magnetic form factor from the right hand side of eq. (33b) we use the identity:

$$1 \equiv \frac{1}{2} \epsilon_{mBl} \epsilon_{mBj} \frac{q_l q_j}{q^2} . \tag{A.9}$$

This can be applied to our expression for the current (44b).

## Figure captions

Fig. 1. The proton electric form factor for the momentum transfers below 1  $GeV$ .

Fig. 2. The neutron electric form factor for the momentum transfers below 1  $GeV$ .

Fig. 3. The proton magnetic form factor normalized to one at  $q^2 = 0$  for the momentum transfers below 1  $GeV$ . The normalization factor can be extracted from table 2.

Fig. 4. The neutron magnetic form factor normalized to one at  $q^2 = 0$  for the momentum transfers below 1  $GeV$ . The normalization factor can be extracted from table 2.

Fig. 5. The isovector charge radius as a function of the box size  $D$  for  $m_\pi = 0$  and  $m_\pi = 139.6 MeV$ .

Fig. 6. The isoscalar electric charge radius as a function of the constituent quark mass  $M$ . The valence and sea parts are marked by the dashed and dashed-dotted lines.

Fig. 7. The isovector electric charge radius as a function of the constituent quark mass  $M$ . The valence and sea parts are marked by the dashed and dashed-dotted lines.

Fig. 8. The electric charge radii of proton and neutron as functions of the constituent quark mass  $M$ . The valence and sea parts are marked by the dashed lines.

Fig. 9. The magnetic moment density of proton and neutron for the constituent quark mass  $M = 420 MeV$ .

This figure "fig1-1.png" is available in "png" format from:

<http://arXiv.org/ps/hep-ph/9312351v1>

This figure "fig2-1.png" is available in "png" format from:

<http://arXiv.org/ps/hep-ph/9312351v1>

This figure "fig3-1.png" is available in "png" format from:

<http://arXiv.org/ps/hep-ph/9312351v1>

This figure "fig1-2.png" is available in "png" format from:

<http://arXiv.org/ps/hep-ph/9312351v1>

This figure "fig2-2.png" is available in "png" format from:

<http://arXiv.org/ps/hep-ph/9312351v1>

This figure "fig3-2.png" is available in "png" format from:

<http://arXiv.org/ps/hep-ph/9312351v1>

This figure "fig1-3.png" is available in "png" format from:

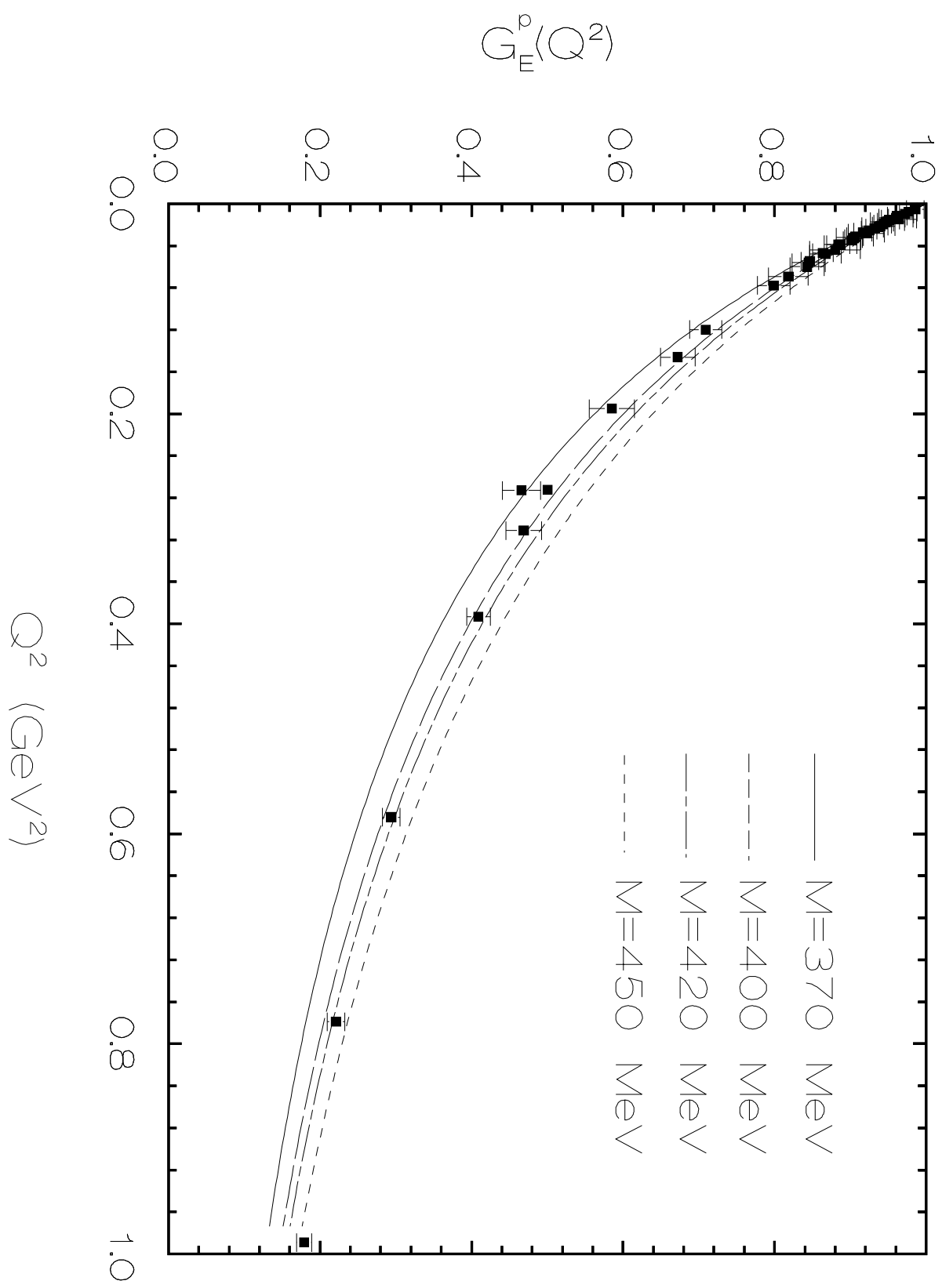
<http://arXiv.org/ps/hep-ph/9312351v1>

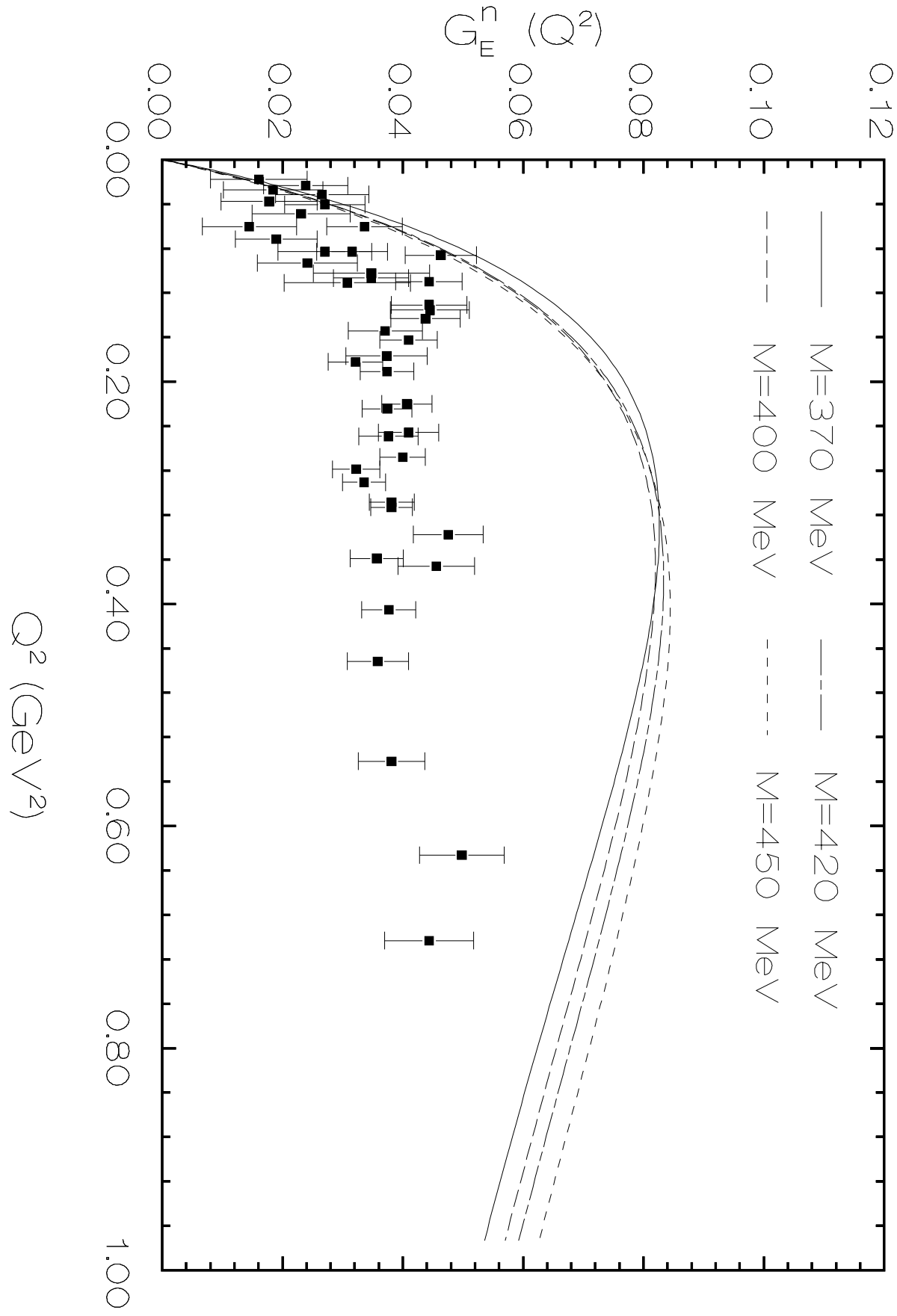
This figure "fig2-3.png" is available in "png" format from:

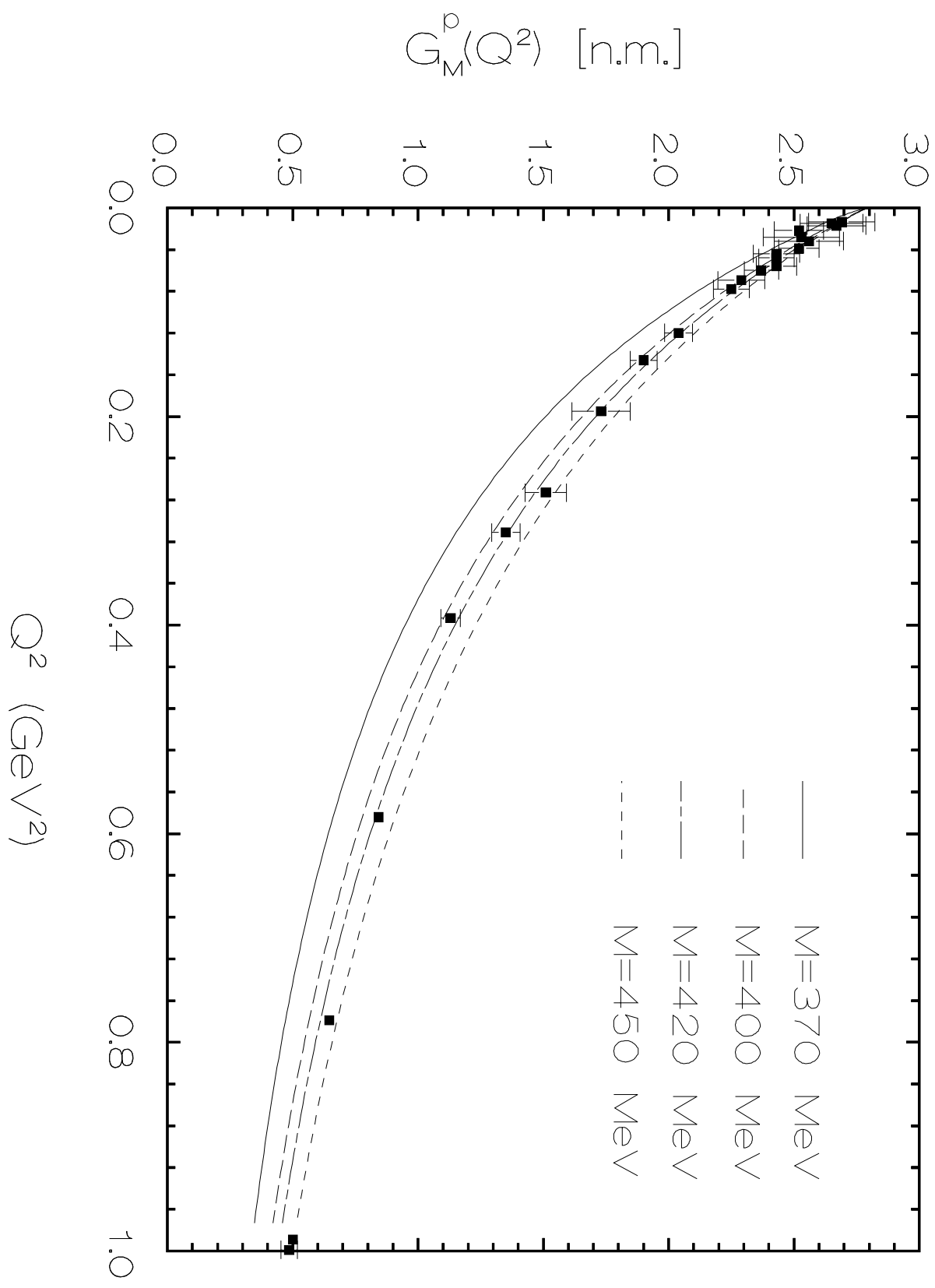
<http://arXiv.org/ps/hep-ph/9312351v1>

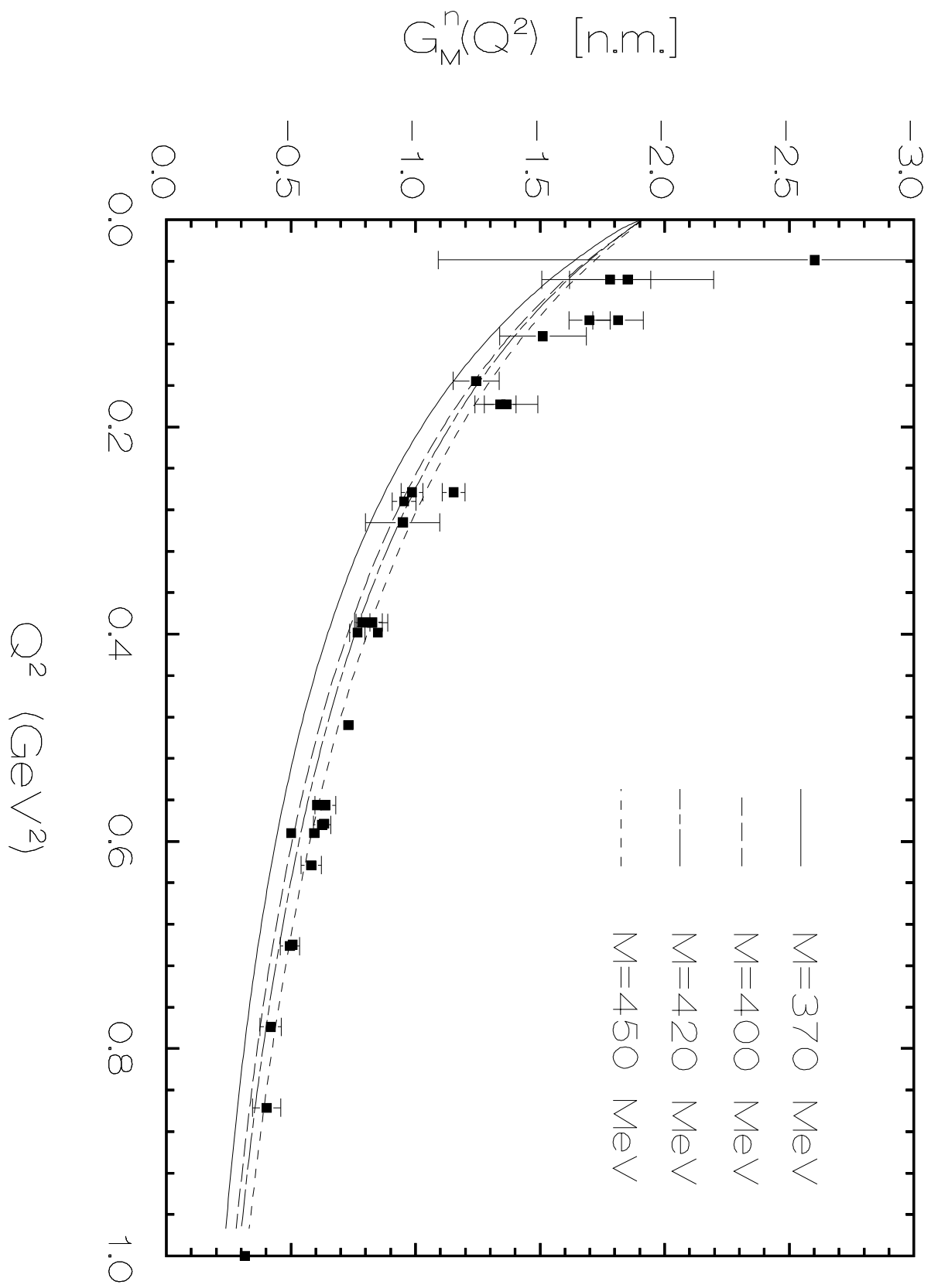
This figure "fig3-3.png" is available in "png" format from:

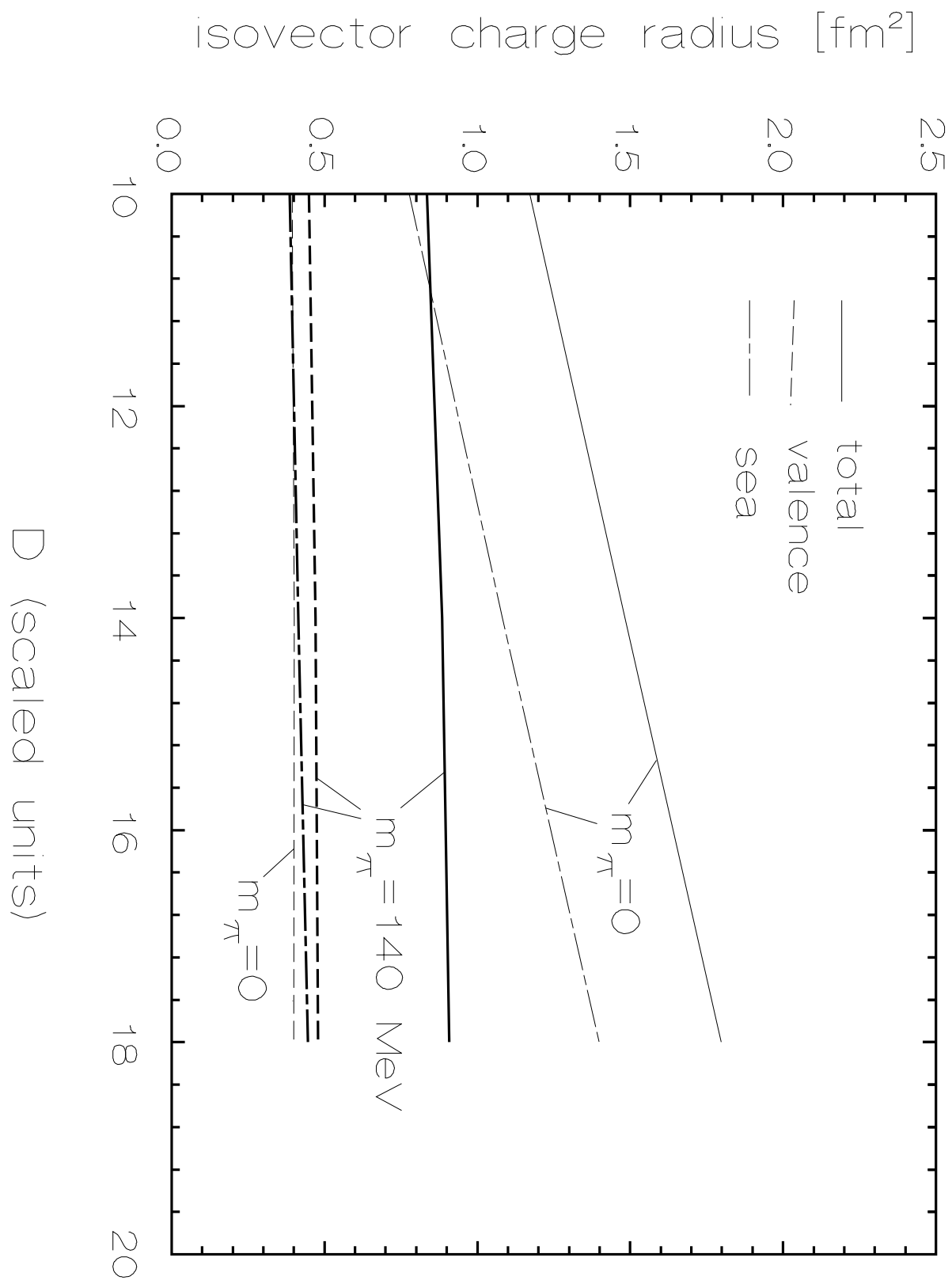
<http://arXiv.org/ps/hep-ph/9312351v1>



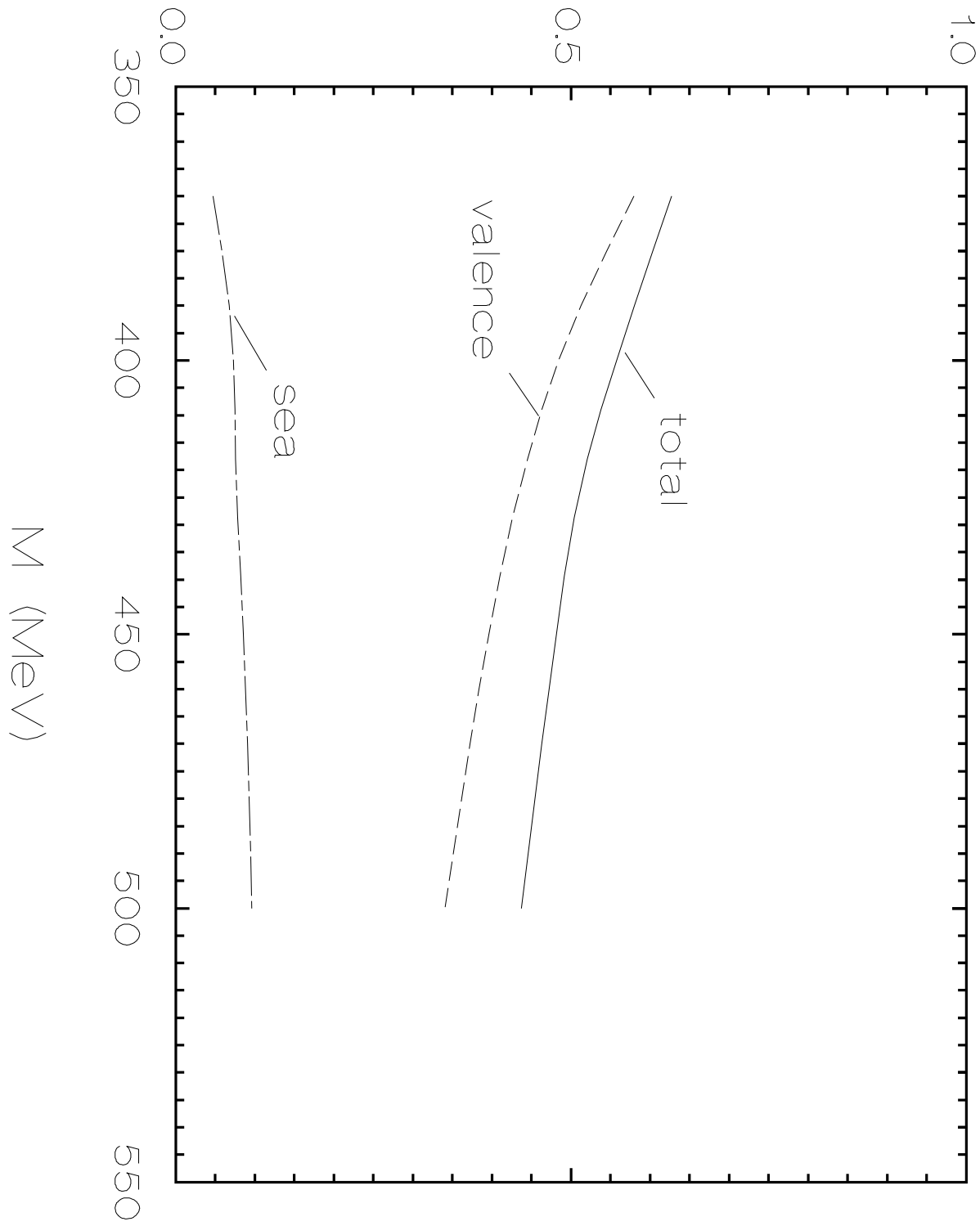




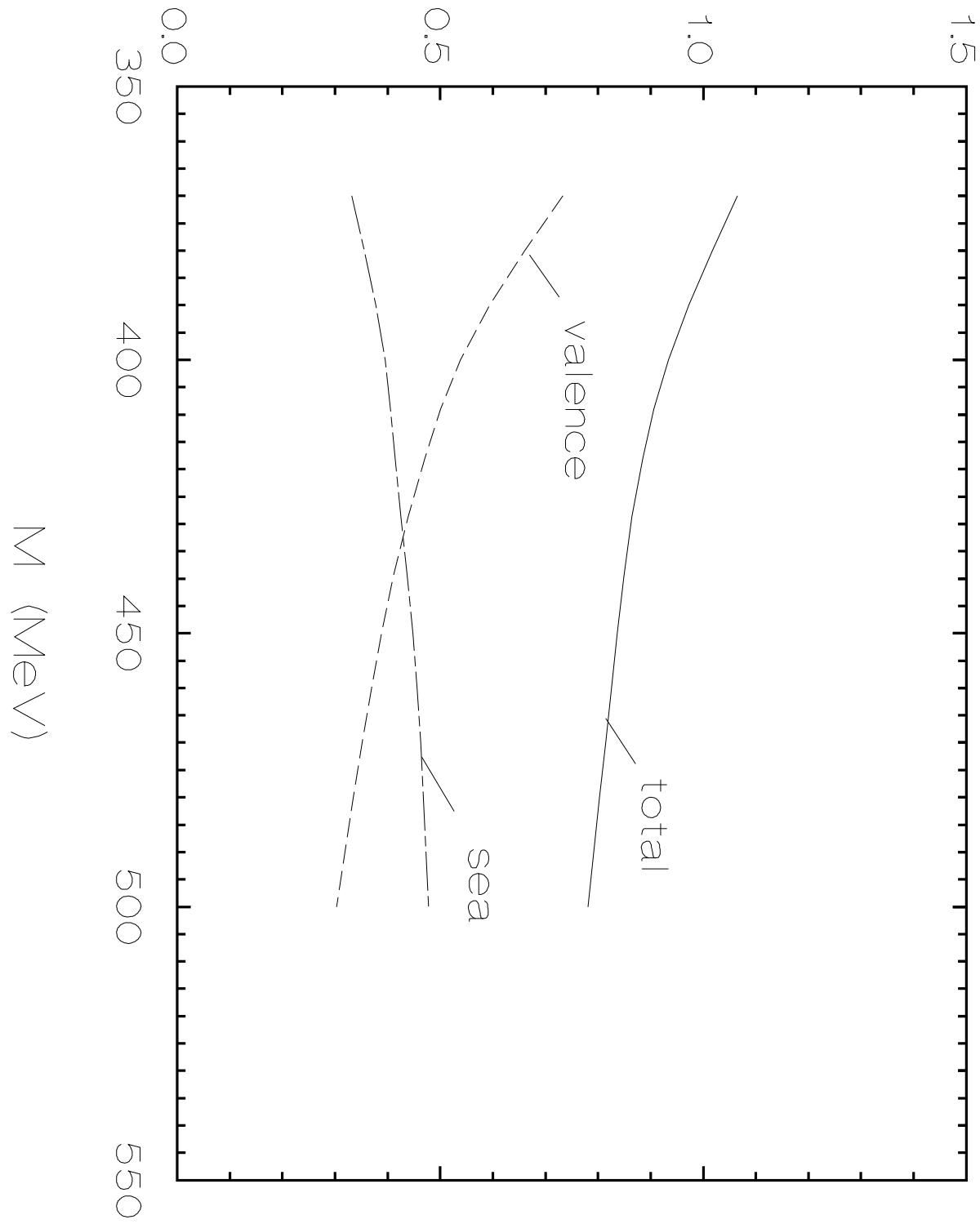




isoscalar charge radius [ $\text{fm}^2$ ]



isovector charge radius [fm<sup>2</sup>]



m.s. charge radii [fm<sup>2</sup>]

